Published in final edited form as:
Neuropathol Appl Neurobiol. 2013 June ; 39(4): 335–347. doi:10.1111/j.1365-2990.2012.01291.x.

LAMINAR DISTRIBUTION OF THE PATHOLOGICAL CHANGES IN SPORADIC FRONTOTEMPORAL LOBAR DEGENERATION WITH TDP-43 PROTEINOPATHY: A QUANTITATIVE STUDY USING POLYNOMIAL CURVE FITTING

Richard A. Armstrong, DPhil[1], **Ronald L. Hamilton, MD**[2], **Ian R. A. Mackenzie, MD**[3], **John Hedreen, MD**[4], **Nigel J. Cairns, PhD**[5,6,7], and **FRCPath**

[1]Vision Sciences, Aston University, Birmingham, UK

[2]Department of Pathology, University of Pittsburgh, Pittsburgh, PA, USA

[3]Department of Pathology, Vancouver General Hospital, Vancouver, Canada

[4]McLean Hospital and Harvard Brain Tissue Resource Center, Belmont, MA, USA

[5]Charles F. & Joanne Knight Alzheimer's Disease Research Center, Washington University School of Medicine, St Louis, Missouri, U.S.A.

[6]Department of Pathology and Immunology Washington University School of Medicine, St Louis, Missouri, U.S.A.

[7]Department of Neurology, Washington University School of Medicine, St Louis, Missouri, U.S.A.

Abstract

Aims—Previous data suggest heterogeneity in laminar distribution of the pathology in the molecular disorder frontotemporal lobar degeneration (FTLD) with transactive response (TAR) DNA-binding protein of 43kDa (TDP-43) proteinopathy (FTLD-TDP). To study this heterogeneity, we quantified the changes in density across the cortical laminae of neuronal cytoplasmic inclusions (NCI), glial inclusions (GI), neuronal intranuclear inclusions (NII), dystrophic neurites (DN), surviving neurons, abnormally enlarged neurons (EN), and vacuoles in regions of the frontal and temporal lobe.

Methods—Changes in density of histological features across cortical gyri were studied in ten sporadic cases of FTLD-TDP using quantitative methods and polynomial curve-fitting.

Results—Our data suggest that laminar neuropathology in sporadic FTLD-TDP is highly variable. Most commonly, NCI, DN, and vacuolation were abundant in the upper laminae and GI, NII, EN, and glial cell nuclei in the lower laminae. TDP-43-immunoreactive inclusions affected more of the cortical profile in longer duration cases, their distribution varied with disease subtype, but was unrelated to Braak tangle score. Different TDP-43-immunoreactive inclusions were not spatially correlated.

Corresponding Author: R.A. Armstrong, Vision Sciences, Aston University, Birmingham, B4 7ET, UK (Tel: 0121-204-4102; Fax: 0121-204-4048; R.A.Armstrong@aston.ac.uk.

The authors report no conflicts of interest.

Contributions of listed authors
Richard Armstrong designed the project, collected the quantitative data, analysed the data, and wrote the manuscript. Nigel Cairns coordinated the project, assisted in project design, contributed cases for the study, and made comments on the manuscript. Ronald Hamilton, Ian Mackenzie, and John Hedreen contributed cases for the study and commented on the manuscript.

Conclusions—Laminar distribution of pathological features in ten sporadic cases of FTLD-TDL is heterogeneous and may be accounted for, in part, by disease subtype and disease duration. In addition, the feed-forward and feed-back cortico-cortical connections may be compromised in FTLD-TDP.

Keywords

Frontotemporal lobar degeneration with TDP-43 proteinopathy (FTLD-TDP); FTLD with ubiquitin-positive inclusions (FTLD-U); Transactive response TAR DNA-binding protein of 43 kDa (TDP-43); Neuronal cytoplasmic inclusions (NCI); Laminar distribution

Introduction

Frontotemporal lobar degeneration (FTLD) is the second most common form of cortical dementia of early-onset after Alzheimer's disease (AD) [1]. The disorder is associated with a heterogeneous group of clinical syndromes including behavioural variant frontotemporal dementia (bvFTD), FTD with motor neuron disease (FTD-MND), progressive non-fluent aphasia (PNFA), semantic dementia (SD), and progressive apraxia (PAX) [2].

FTLD with transactive response (TAR) DNA-binding protein of 43kDa (TDP-43) proteinopathy (FTLD-TDP), previously called FTLD with ubiquitin-immunoreactive inclusions (FTLD-U) [3,4], is characterized by a variable neocortical and allocortical atrophy principally affecting the frontal and temporal lobes. In addition, there is neuronal loss, microvacuolation largely affecting the superficial cortical laminae, and a reactive astrocytosis [5,6]. A variety of TDP-43-immunoreactive inclusions are present including neuronal cytoplasmic inclusions (NCI), neuronal intranuclear inclusions (NII), dystrophic neurites (DN), and glial inclusions (GI) [6]. Based on the distribution and density of inclusions, there have been attempts to classify FTLD-TDP into subtypes [7–10]. Most schemes define four pathological subtypes, based originally on ubiquitin immunohistochemistry (IHC) but extended to cases of FTLD-TDP, and which utilize the distribution and density of the pathological changes in neocortical regions. The same descriptors have been used to define subtypes but the numbering of each subtype varies between different schemes. Using a consensus system proposed by Cairns et al. [10] and based on both genetics and previous schemes: type 1 cases (Mackenzie-type 2) are characterized by long DN in superficial cortical laminae with few or no NCI or NII, type 2 (Mackenzie-type 3) by numerous NCI in superficial and deep cortical laminae with infrequent DN and sparse or no NII, type 3 (Mackenzie-type 1) by pathology predominantly affecting the superficial cortical laminae with numerous NCI, DN and varying numbers of NII, and type 4 by numerous NII, and infrequent NCI and DN especially in neocortical areas. Although there may be no clear distinction between the various subtypes [6], it is still possible that there are different distribution patterns of pathology that characterize FTLD.

In many neurodegenerative disorders, the density of pathological inclusions varies significantly across the cortical laminae from pia mater to white matter [11–15]. The laminar distribution of an inclusion may reflect degeneration of neural pathways that have their cells of origin or axon terminals located within one or more laminae and can therefore indicate the pattern of cortical degeneration in a disorder [16,17]. Previous studies based on subjective and semi-quantitative estimates of inclusion density, suggest heterogeneity in laminar distribution of the pathology in FTLD-TDP [7–10] but these differences have not been systematically investigated using quantitative methods. To study this heterogeneity, we quantified the changes in density across the cortical laminae of the TDP-43-immunoreactive inclusions, abnormally enlarged neurons (EN), surviving neurons, vacuoles, and glial cell nuclei in gyri of frontal and temporal cortex in ten cases of the disease. Quantitative

methods and a polynomial curve-fitting procedure [18] were used to study changes in density of each histological feature across the gyri. The specific objectives were: (1) to describe the changes in density of histological features across the laminae, (2) to determine whether the distribution of the TDP-43-immunoreactive inclusions was correlated with disease duration, stage of disease, and consistent with previously assigned disease subtypes, and (3) to determine the spatial correlations of the pathological features.

Materials and methods

Cases

Ten cases of sporadic FTLD-TDP (see Table 1) were obtained from dementia centers in the USA and Canada: Vancouver General Hospital, Vancouver, Canada (5 cases), University of Pittsburgh, Pittsburgh, PA (3 cases), and Harvard Brain Tissue Resource Center, Belmont, MA (2 cases). All cases were without a family history of neurodegenerative disease and none had mutations in genes known to cause TDP-43 proteinopathy, viz., *progranulin* (*GRN*) [19–24], *valosin-containing protein* (*VCP*) [25], *TAR DNA-binding protein (TARDBP)* [26–29], or *C90RF72* [30, 31]. All cases exhibited FTLD with neuronal loss, microvacuolation of the superficial cortical laminae, and a reactive astrocytosis consistent with proposed diagnostic criteria for FTLD-TDP [10]. A variety of TDP-43-immunoreactive inclusions was present including NCI, NII, DN, and GI consistent with a diagnosis of TDP-43 proteinopathy [10]. One case had coexisting motor neuron disease (FTLD-MND) [32,33] but none met 'Consortium to Establish a Registry of Alzheimer's Disease' (CERAD) [34], 'National Institute on Aging (NIA)-Reagan Institute' criteria [35,36], or NIA-Alzheimer's Association Guidelines [37] for a neuropathological diagnosis of Alzheimer's disease (AD) and none had associated hippocampal sclerosis (HS). Staging of cases was based on the Braak tangle score [38]. Cases had been assigned previously to the four proposed subtypes of FTLD-TDP by an experienced neuropathologist using the composite ('harmonized') scheme of Cairns et al. [10]. Only subtypes 1, 2 and 3 were represented in the present sample as subtype 4 may be more frequently associated with familial FTLD-TDP with *VCP* gene mutation [25].

Histological methods

After death, the consent of the next of kin was obtained for brain removal following local Ethical Committee procedures and the 1995 Declaration of Helsinki (as modified Edinburgh, 2000). Tissue blocks were taken from the frontal lobe at the level of the genu of the corpus callosum to study the middle frontal gyrus (MFG) and the temporal lobe at the level of the lateral geniculate body to study the inferior temporal gyrus (ITG), and parahippocampal gyrus (PHG). Tissue was fixed in 10% phosphate buffered formal-saline and embedded in paraffin wax. Following formic acid (95%) pretreatment for 5 minutes, IHC was performed on 4 – 10μm sections with a rabbit polyclonal antibody that recognizes physiologic TDP-43 epitopes (dilution 1:1000; ProteinTech Inc., Chicago, IL). Sections were also stained with haematoxylin.

Morphometric methods

In gyri with sufficient densities of inclusions, the distribution of the NCI, GI, NII, and DN together with the surviving neurons, EN, vacuoles, and glial cell nuclei was studied from pia mater to white matter using methods described previously [39]. TDP-immunoreactive pathology is not distributed evenly along the gyri. Hence, five traverses from pia mater to the edge of the white matter were located randomly along each gyrus. All histological features were then counted in 50 × 250μm sample fields arranged contiguously, the larger dimension of the field being located parallel with the surface of the pia mater. An eye-piece micrometer comprised the sample field and was moved down each traverse one step at a

time from pia mater to the edge of the white matter. Histological features of the section were used to correctly position the field.

The NCI were rounded, spicular, or skein-like [6,40,41], while the GI morphologically resembled the 'coiled bodies' reported in tauopathies such as corticobasal degeneration (CBD) [42,43], progressive supranuclear palsy (PSP) [44–46], and argyrophilic grain disease (AGD) [47]. The NII were lenticular, spindle-shaped, or circular in shape [6,48] and the DN were long and contorted [6,49]. It can be difficult to identify surviving neurons without special stains. Hence, surviving neurons were identified in the TDP-43 sections as cells containing at least some stained cytoplasm in combination with larger shape and non-spherical outline [50]. All perikarya meeting these criteria were counted not just the pyramidal cells. Small spherical or asymmetrical nuclei without cytoplasm, but with the presence of a thicker nuclear membrane and more heterogeneous chromatin, were identified as glial cells. EN had enlarged perikarya, lacked NCI, had a shrunken nucleus displaced to the periphery of the cell, and a maximum cell diameter at least three times that of the nucleus [50]. The number of discrete vacuoles that were greater than 5μm in diameter was also counted in each sample field [51,52]. It can be difficult to differentiate microvacuolation of the neuropil from vacuolation around neurons and blood vessels attributable to artifacts of processing. Hence, vacuoles clearly associated with such structures were not counted. The mean of the counts from the five traverses was calculated to study variations in density of each histological feature across the gyrus.

Data analysis

No attempt was made to locate precisely the boundaries between individual cortical laminae. First, the degree of cortical degeneration present in many gyri made laminar identification difficult. Second, identification was especially difficult in the frontal cortex because it exhibits a heterotypical structure, i.e., six laminae cannot always be clearly identified and vary in prominence from case to case. Third, inclusions appeared to exhibit complex patterns of distribution across the cortex rather than being confined to specific laminae. Hence, variations in lesion density with distance across the cortex were analyzed using a polynomial curve-fitting procedure (STATISTICA software, Statsoft Inc., 2300 East 14th St, Tulsa, OK, 74104, USA) [11,18,53]. For each gyrus, polynomials were fitted successively to the data. Hence, quadratic curves are parabolic, cubic curves are 'S' shaped and quartic curves often appear as 'double-peaked' or 'bimodal'. With each fitted polynomial, the correlation coefficients (Pearson's 'r'), regression coefficients, standard errors (SE), values of t, and the residual mean square were obtained [18]. At each stage, the reduction in the sums of squares (SS) was tested for significance. The analysis was continued until either a non-significant value of F was obtained or there was little gain in the explained variance [18]. Polynomials greater than the fourth order did not fit any of the distributions. The shape of the fitted polynomial curve was used to classify the distribution of each histological feature across the cortex. Hence, histological features exhibiting a single peak of density were described as 'unimodal', peak density being located either in the upper (approximating to laminae I,II,III) or lower (approximating to laminae V,VI) cortex while those with two peaks as 'bimodal', peaks of density occurring in the upper and lower cortex. These histological features were then classified further according to whether the density peaks were of similar or different magnitude in upper and lower cortex. To examine the relationship between laminar distribution, disease duration, Braak tangle stage [38], and disease subtype [7–10], the frequencies of the different types of distribution exhibited by the TDP-43-immunoreactive inclusions were compared using chi-square (χ^2) contingency table tests.

To determine the degree to which different histological features occurred within the same or different regions of the cortex or were distributed independently of each other, correlations

between the densities of all histological features were tested using Pearson's correlation coefficient ('r').

Results

Examples of the distribution of the pathology in sporadic FTLD-TDP cases are shown in Figs 1 and 2. Fig 1 shows extensive vacuolation in the ITG, typically present in the superficial laminae of many gyri, while Fig 2 shows TDP-43-immunoreactive inclusions in the upper laminae of the ITG.

Examples of the changes in density of NCI and NII across the cortex and the curve-fitting procedure are shown in Fig 3. The distribution of NCI in the MFG of case D was fitted by a third-order polynomial ($r = 0.70$, $P < 0.001$), a large density peak being present in the upper cortex, and significantly lower densities of NCI in the lower cortex. The distribution of NII in the ITG of case F was also fitted by a third-order polynomial ($r = 0.65$, $P < 0.01$). The distribution of the NII overlapped with the NCI, but the greatest densities of NII occurred in the lower cortex.

Examples of the distribution of surviving neurons and vacuoles are shown in Fig 4. The distribution of surviving neurons in the MFG of case B was fitted by a fourth-order polynomial ($r = 0.61$, $P < 0.01$) indicating a bimodal distribution, i.e., the distribution was double-peaked, densities in the upper laminae being slightly greater, with the exception of a single datum point, than those in the lower laminae. The distribution of the vacuoles in the PHG of case A was fitted by a second-order polynomial ($r = 0.96$, $P < 0.001$). Hence, although some vacuolation is evident throughout the cortical profile, the density of the vacuoles was greatest in the superficial laminae declining markedly with distance across the cortex.

The results of the curve fitting procedure for each histological feature in all gyri studied are shown in Table 2 and a summary of these distributions in Table 3. The NCI were distributed largely in the upper laminae in 7/23 (30%) of gyri studied and in further 8 gyri, a bimodal distribution was present, the density peak in the upper cortex being larger or of similar magnitude to that in the lower cortex. In 6/23 (26%) gyri, there was no significant change in the density of NCI across the cortex. In 4/6 (67%) gyri, the density of GI was greatest in the lower cortex. Similarly, the NII frequently exhibited greater densities in the lower cortex, 11/21 (52%) gyri showing this pattern. In addition, NII exhibited a smaller density peak in the upper cortex and in 8 gyri, there were no differences in NII density across the cortex. In 6/13 (46%) gyri, the density of DN was greatest in the upper cortex. The density of the EN was greatest in the lower cortex in 6/20 (30%) gyri but in the remaining gyri, EN were more uniformly distributed across the cortex. The distribution of the surviving neurons was highly variable. In 17/30 (57%) gyri, the distribution of the surviving neurons was bimodal, the density in the upper cortex being either greater than or similar to that in the lower cortex. In 8 gyri, there were no significant differences in the density of surviving neurons across the cortex. The greatest density of the vacuolation was present in the upper cortex, 25/30 (83%) gyri showing this pattern. In 17/30 (57%) of these gyri, the vacuoles also exhibited a smaller density peak in the lower cortex. Glial cell nuclei were more abundant in the lower cortex and in many gyri, glial cell density increased linearly across the cortex from pia mater to white matter. There were no consistent differences in the distribution of histological features between gyri of the frontal and temporal cortex, or in the case with associated MND compared with the cases without MND.

The relationship between the distribution of the TDP-43-immunoreactive inclusions, disease duration, and Braak tangle stage is shown in Table 4. Inclusions affecting either upper or

lower cortex alone were more frequent in shorter duration cases while bimodal distributions affecting upper and lower cortex were more frequent in longer duration cases ($\chi^2 = 10.63$, 4DF, $P < 0.05$). There were no significant differences in the frequencies of laminar distribution when cases were classified according to Braak tangle stage ($\chi^2 = 9.46$, 6DF, $P > 0.05$).

The relationship between the distributions of NCI, NII, and DN and previously assigned disease subtypes is shown in Table 5. In cases assigned to subtype 1, NCI and NII were relatively infrequent while DN were more abundant and more commonly distributed in the upper cortex. In cases assigned to subtype 2, pathology affected both the upper and lower cortices and NCI and DN were abundant either in the upper cortex alone or a bimodal distribution was present, inclusions being present in both upper and lower cortices, and with NII predominant in the lower cortex. In cases assigned to subtype 3, the TDP-43-immunoreactive inclusions were predominantly located in the upper cortex.

A summary of the spatial correlations between the densities of the various histological features across the cortex is shown in Table 5. In the majority of gyri, there were no significant spatial correlations between the different TDP-43-immunoreactive inclusions. NCI density was positively correlated with surviving neuron density in 9/24 (38%) gyri and surviving neuron and vacuole densities were positively correlated in 14/31 (45%) gyri. Vacuoles and glial cell nuclei densities were negatively correlated in 12/30 (40%) gyri.

Discussion

Both phosphorylation-dependent (pTDP-43) and independent (iTDP-43) antibodies have been used to study TDP-43- immunoreactive pathological changes in FTLD-TDP [54–58]. Initially many groups used iTDP-43 which immunolabels normal physiological TDP-43 as well as pathological inclusions. This is a particularly useful attribute as this antibody shows clearly that in most neurons there is reduced staining in the nucleus and increased staining of the cytoplasm leading to the hypothesis that the protein is abnormally translocated in disease. However, it is often difficult to distinguish the presence of an abnormal inclusion, or pre-inclusion, in the nucleus, or even the cytoplasm where normal and abnormal staining may admix. The advantage of pTDP-43 antibodies is that they do not immunolabel normal physiological TDP-43 [54,56], especially in the nucleus, thus enabling the TDP-43-immunoreactive lesions to be more clearly visualized and quantified. In a previous study [58], we compared he densities of TDP-43-immunoreactive inclusions using iTDP-43 and pTDP-43 antibodies. On average, the pTDP-43 antibody revealed slightly more NCI and GI per sample field than iTDP-43 while on average pTDP-43 revealed slightly fewer NII than the iTDP-43 antibody. For the DN, very similar densities of DN were revealed by both antibodies. Hence, although there are some differences in density revealed by both types of antibody, these differences are unlikely to significantly affect the laminar distributions as revealed by the present iTDP-43 antibody.

The data suggest significant changes in density of histological features across the cortex in sporadic FTLD-TDP. Changes in density were variable with significant differences between gyri and cases. The most consistent patterns of distribution were: (1) significant vacuolation was present in the superficial laminae, declining in importance with distance below the pia mater and (2) a greater abundance of glial cell nuclei in the lower cortex. Of the TDP-43-immunoreactive inclusions, the NCI and DN were most frequently abundant in the upper cortex and NII and GI in the lower cortex. The quantitative data support some aspects of the classification of cases into subtypes based on subjective and semi-quantitative assessment of the pathology [7–10]. Hence, DN and NCI were more frequent in the superficial cortical laminae especially in cases assigned to subtypes 1 and 3. In addition, numerous NCI were

present in superficial and deep cortical laminae in cases assigned to subtype 2. Hence, previously reported differences associated with disease subtype [7–10] could account for some of the variation in laminar distribution observed between the 10 cases. However, a much larger series of cases would need to be studied to establish whether different subtypes consistently exhibit a specific laminar distribution of inclusions. If this hypothesis is shown to be correct, it raises the possibility that different anatomical pathways may be affected in the various subtypes. Hence, both the feedforward and feedback cortico-cortical pathways may be affected in subtype 2 while the feedforward pathways may be predominantly affected in subtypes 1 and 3.

Distribution across the cortex was also related to disease duration, inclusions in shorter duration cases being more likely to be unimodal and restricted either to upper or lower laminae, while a bimodal distribution was more common in longer duration cases. These data suggest that as the disease progresses, inclusions could spread vertically within modules or columns to affect more of the cortical profile.

The distribution of the surviving neurons was especially variable in our cases. In normal elderly brain, pyramidal neurons in frontal and temporal cortex often exhibit a bimodal distribution in which peak density in the upper cortex (corresponding to laminae II/III) is often larger than in the lower cortex (corresponding to laminae V/VI) [17]. A similar bimodal distribution was observed in some gyri in FTLD-TDP, but in eight gyri, peak densities were similar in the upper and lower cortex, and in eight further gyri, surviving neurons were uniformly distributed down the cortex consistent with greater neuronal loss in the upper cortex. Pathological changes in the upper cortex could be associated with degeneration of the feed-forward cortico-cortical projections, which have their cells or origin in laminae II/III as shown in other disorders [16]. By contrast, EN, which may reflect either a stress response [58] or axonal degeneration [60,61], and glial cell nuclei were more abundant in the lower cortex consistent with degeneration of the lower laminae in FTLD-TDP. Pathological changes in lower cortex could result from degeneration of either the feed-back cortico-cortical projections [16] or the afferent and efferent cortical-subcortical projections. As in other neurodegenerative disorders, it is possible that the pathology spreads between cortical regions via cell to cell contact [16,62] and observed variations in laminar distribution between cases and gyri could represent different stages of this process.

The various TDP-43-immunoreactive inclusion were not spatially correlated in the majority of gyri suggesting that NCI, NII, DN, and GI do not affect the same cortical laminae. NCI and surviving neuron densities, however, were positively correlated in over a third of gyri suggesting that a constant proportion of all surviving neurons develop NCI in some gyri. Vacuole and surviving neuron densities were also positively correlated in nearly half of the gyri studied. Vacuolation also occurs in Creutzfeldt-Jakob disease (CJD), dementia with Lewy bodies (DLB), and advanced AD [6]. In sporadic CJD (sCJD), for example, vacuoles are often clustered around neuronal perikarya [51] and in the cerebellum of variant CJD (vCJD), clusters of vacuoles in the molecular layer are negatively correlated with surviving Purkinje cells [52]. Hence, the relationship between surviving neurons and vacuolation is complex. An initial positive correlation may arise if vacuoles develop in association with the dendrites of degenerating neurons. However, if the neuronal perikarya subsequently disappear but the vacuoles remain or *vice versa*, a negative correlation may result. Vacuolation within the superficial cortical laminae in FTLD-TDP could be the result of neuronal degeneration within laminae II/III subsequently affecting the ascending projections. Variation in correlation in different gyri could reflect the stage of the disease, e.g., a positive correlation between surviving neurons and vacuolation might disappear as significantly more neurons are lost. Vacuole and glial cell densities were negatively

correlated in approximately half the gyri studied reflecting their relative abundance in the upper and lower laminae respectively.

In conclusion, no single pattern of laminar distribution is characteristic of the pathology of the ten sporadic FTLD-TDP cases studied. Most commonly, the pathology affected all laminae with significant vacuolation of the superficial cortical laminae and a gliosis largely affecting the lower laminae. Of the TDP-43-immunoreactive inclusions, most frequently the NCI and DN were abundant in the upper cortex and NII and GI in the lower cortex. Variations in laminar distribution of the TDP-43 immunoreactive inclusions may be explained in part by disease subtype and disease duration, the latter reflecting stages in the spread of the pathology possibly via the feed-forward and feed-back cortico-cortical projections.

Acknowledgments

We thank clinical, genetic, pathology, and technical staff of Vancouver General Hospital, Vancouver, Canada; University of Pittsburgh, Pittsburgh, PA; and Harvard Brain Tissue Resource Center, Belmont, MA for making information and tissue samples available for this study and we thank the families of patients whose generosity made this research possible. Support for this work was provided by the National Institute on Aging of the National Institutes of Health to NJC (P50-AG05681, and P01-AG03991) and to RH (P50-AG05133).

List of abbreviations

AD	Alzheimer’s disease
AGD	Argyrophilic grain disease
CBD	Corticobasal degeneration
CERAD	'Consortium to Establish a Registry of Alzheimer's Disease'
DN	Dystrophic neurites
EN	Abnormally enlarged neurons
FTD	Frontotemporal dementia
FTLD	Frontotemporal lobar degeneration
FTLD-U	Frontotemporal lobar degeneration with ubiquitin positive inclusion
GI	Glial inclusions
GL	Glial cell nuclei
GRN	*Progranulin* gene
IHC	Immunohistochemistry
ITG	Inferior temporal gyrus
MFG	Middle frontal gyrus
MND	Motor neuron disease
NCI	Neuronal cytoplasmic inclusion
NIA	National Institute on Aging
NII	Neuronal intranuclear inclusion
NFT	Neurofibrillary tangle
PAX	Progressive apraxia

PHG	Parahippocampal gyrus
PNFA	Progressive non-fluent aphasia
PiD	Pick's disease
PSP	Progressive supranucuclear palsy
SD	Semantic dementia
SP	Senile plaque
STG	Superior temporal gyrus
TARDBP	TAR DNA-binding protein
TDP-43	Transactive response (TAR) DNA-binding protein of 43kD
VCP	Valosin-containing protein

References

1. Tolnay M, Probst A. Frontotemporal lobar degeneration- tau as a pied piper. Neurogenetics. 2002; 4:63–75. [PubMed: 12481984]
2. Snowden J, Neary D, Mann D. Frontotemporal lobar degeneration: clinical and pathological relationships. Acta Neuropathol. 2007; 114:31–38. [PubMed: 17569065]
3. Woulfe J, Kertesz A, Munoz DG. Frontotemporal dementia with ubiquinated cytoplasmic and intranuclear inclusions. Acta Neuropathol. 2001; 102:94–102. [PubMed: 11547957]
4. Kovari E, Gold G, Giannakopoulos P, Bouras C. Cortical ubiquitin positive inclusions in frontotemporal dementia without motor neuron disease: a quantitative immunocytochemical study. Acta Neuropathol. 2004; 108:207–212. [PubMed: 15170577]
5. Cairns NJ, Neumann M, Bigio EH, Holm IE, Troost D, Hatanpaa KJ, Foong C, White CL III, Schneider JA, Kretzschmar HA, Carter D, Taylor-Reinwald L, Paulsmeyer K, Strider J, Gitcho M, Goate AM, Morris JC, Mishra M, Kwong LK, Steiber A, Xu Y, Forman MS, Trojanowski JQ, Lee VMY, Mackenzie IRA. TDP-43 familial and sporadic frontotemporal lobar degeneration with ubiquitin inclusions. Am J Pathol. 2007a; 171:227–240. [PubMed: 17591968]
6. Armstrong RA, Ellis W, Hamilton RL, Mackenzie IRA, Hedreen J, Gearing M, Montine T, Vonsattel J-P, Head E, Lieberman AP, Cairns NJ. Neuropathological heterogeneity in frontotemporal lobar degeneration with TDP-43 proteinopathy: a quantitative study of 94 cases using principal components analysis. J Neural Transm. 2010; 117:227–239. [PubMed: 20012109]
7. Mackenzie IR, Baborie A, Pickering-Brown S, Du Plessis D, Jaros E, Perry RH, Neary D, Snowden JS, Mann DMA. Heterogeneity of ubiquitin pathology in frontotemporal lobar degeneration: classification and relation to clinical phenotype. Acta Neuropathol. 2006a; 112:539–549. [PubMed: 17021754]
8. Sampathu DM, Neumann M, Kwong LK, Chou TT, Micsenyi M, Truax A, Bruce J, Grossman M, Trojanowski JQ, Lee VM. Pathological heterogeneity of frontotemporal lobar degeneration with ubiquitin-positive inclusions delineated by ubiquitin immunohistochemistry and novel monoclonal antibodies. Am J Pathol. 2006; 169:1343–1352. [PubMed: 17003490]
9. Neumann M, Igaz LM, Kwong LK, Nakashima-Yasuda H, Kolb SJ, Dreyfuss G, Kretzschmar HA, Trojanowski JQ, Lee VMY. Absence of heterogeneous nuclear riboproteins and survival neuron protein (TDP-43) positive inclusions in frontotemporal lobar degeneration. Acta Neuropathol. 2007; 113:543–548. [PubMed: 17415574]
10. Cairns NJ, Bigio EH, Mackenzie IRA, Neumann M, Lee VMY, Hatanpaa KJ, White CL, Schneider JA, Grinberg LT, Halliday G, Duyckaerts C, Lowe JS, Holm IE, Tolnay M, Okamoto K, Yokoo H, Murayama S, Woulfe J, Munoz DG, Dickson DW, Ince PG, Trojanowski JQ, Mann DMA. Neuropathologic diagnostic and nosological criteria for frontotemporal lobar degeneration: consensus of the Consortium for Frontotemporal Lobar Degeneration. Acta Neuropathol. 2007b; 114:5–22. [PubMed: 17579875]

11. Armstrong RA. β-amyloid (Aβ) deposits and blood vessels: laminar distribution in the frontal cortex of patients with Alzheimer's disease. Neurosci Res Communs. 1996a; 18:19–28.
12. Armstrong RA, Cairns NJ, Lantos PL. Laminar distribution of cortical Lewy bodies and neurofibrillary tangles in dementia with Lewy bodies. Neurosci Res Commun. 1997; 21:145–152.
13. Armstrong RA, Cairns NJ, Lantos PL. Laminar distribution of Pick bodies, Pick cells, and Alzheimer's disease pathology in the frontal and temporal cortex in Pick's disease. Neuropathol Appl Neurobiol. 1999; 25:266–271. [PubMed: 10476043]
14. Armstrong RA, Lantos PL, Cairns NJ. Laminar distribution of ballooned neurons and tau positive neurons with inclusions in patients with corticobasal degeneration. Neurosci Res Communs. 2000; 27:85–93.
15. Armstrong RA, Lantos PL, Cairns NJ. Multiple system atrophy: laminar distribution of the pathological changes in frontal and temporal neocortex. Clin Neuropathol. 2005; 24:230–235. [PubMed: 16167547]
16. De Lacoste M, White CL. The role of cortical connectivity in Alzheimer's disease pathogenesis: a review and model system. Neurobiol Aging . 1993; 14:1–16. [PubMed: 8450928]
17. Armstrong RA, Slaven A. Does the neurodegeneration of Alzheimer's disease spread between visual cortical regions B17 and B18 via the feedforward or feedback short cortico-cortical projections. Neurodegen. 1994; 3:191–196.
18. Armstrong, RA.; Hilton, A. Statistical Analysis in Microbiology: Statnotes. Hoboken, NJ, USA: Wiley-Blackwell; 2011.
19. Baker M, Mackenzie IR, Pickering-Brown SM, Gass J, Rademakers R, Lindholm C, Snowden J, Adamson J, Sadovnick AD, Rollinson S, Cannon A, Dwosh E, Neary D, Melquist S, Richardson A, Dickson D, Berger Z, Eriksen J, Robinson T, Zehr C, Dickey CA, Crook R, McGowan E, Mann D, Boeve B, Feldman H, Hutton M. Mutations in progranulin cause tau-negative frontotemporal dementia linked to chromosome 17. Nature. 2006; 442:916–919. [PubMed: 16862116]
20. Cruts M, Gijselink I, van der Zee J, Engelborgs S, Wils H, Pirici D, Radamakers R, Vandenberghe R, Dermaut B, Martin JJ, van Duijn C, Peeters K, Sciot R, Santens P, De pooter T, Mattheijssens M, van den BM, Cuijt I, Vennekens K, De Deyn PP, Kumar-Singh S, Van Broeckhoven C. Null mutations in progranulin cause ubiquitin-positive frontotemporal dementia linked to chromosome 17q21. Nature. 2006; 442:920–924. [PubMed: 16862115]
21. Mukherjee O, Pastor P, Cairns NJ, Chakraaverty S, Kauwe JSK, Shears S, Behrens MI, Budde J, Hinrichs AL, Norton J, Levitch D, Taylor-Reinwald L, Gitcho M, Tu PH, Grinberg LT, Liscic RM, Armendariz J, Morris JC, Goate AM. HDDD2 is a familial frontotemporal lobar degeneration with ubiquitin-positive tau-negative inclusions caused by a missense mutation in the signal peptide of progranulin. Annals of Neurology. 2006; 60:314–322. [PubMed: 16983685]
22. Mackenzie IRA, Baker M, Pickering-Brown S, Hsinng GYR, Lindholm C, Dwosh E, Cannon A, Rademakers R, Hutton M, Feldman HH. The neuropathology of frontotemporal lobar degeneration caused by mutations in the progranulin gene. Brain. 2006b; 129:3081–3090. [PubMed: 17071926]
23. Rademakers R, Hutton M. The genetics of frontotemporal lobar degeneration. Curr Neurol Neurosci Rep. 2007; 7:434–442. [PubMed: 17764635]
24. Behrens MI, Mukherjee O, Tu PH, Liscic RM, Grinberg LT, Carter D, Paulsmeyer K, Taylor-Reinwald L, Gitcho M, Norton JB, Chakraverty S, Goate AM, Morris JC, Cairns NJ. Neuropathologic heterogeneity in HDDD1: a familial frontotemporal lobar degeneration with ubiquitin-positive inclusions and progranulin mutation. Alz Dis Assoc Disord. 2007; 21:1–7.
25. Forman MS, Mackenzie IR, Cairns NJ, Swanson E, Boyer PJ, Drachman DA, Jhaveri BS, Karlawish JH, Pestrvik A, Smith TN, Tu PH, Watts GDJ, Markesbery WR, Smith CD, Kimonis VE. Novel ubiquitin neuropathology in frontotemporal dementia with valosin-containing protein gene mutations. J Neuropathol Exp Neurol. 2006; 65:571–581. [PubMed: 16783167]
26. Gitcho MA, Baloh RH, Chakraverty S, Mayo K, Norton JB, Levitch D, Hatanpaa K, J, White C L III, Bigio EH, Caselli R, Baker M, Al-Lozi MT, Morris JC, Pestronk A, Rademakers R, Goate AM, Cairns NJ. TDP-43 A315T mutation in familial motor neuron disease. Ann Neurol. 2008; 63:535–538. [PubMed: 18288693]
27. Kabashi E, Valdmanis PN, Dion P, Spiegelman D, McConkey BJ, Vande Velde C, Bouchard J.-P, Lacomblez L, Pochigaeva K, Salachas F, Pradat P-F, Camu W, Meininger V, Dupre N, Rouleau

GA. TARDBP mutations in individuals with sporadic and familial amyotrophic lateral sclerosis. Nature Genet. 2008; 40:572–574. [PubMed: 18372902]

28. Benajiba L, Le Ber I, Camuzat A, Lacoste M, Thomas-Anterion C, Couratier P, Legallic S, Salachas F, Hannequin D, Decousus M, Lacomblez L, Guedj E, Golfier V, Camu W, Dubois B, Campion D, Meininger V, Brice A. French Clinical and Genetic Research Network on Frontotemporal Lobar Degeneration/Frontotemporal Lobar Degeneration with Motoneuron Disease TARDBP mutations in motoneuron disease with frontotemporal lobar degeneration. Ann Neurol. 2009; 65:470–474. [PubMed: 19350673]
29. Gitcho MA, Bigio EH, Mishra M, Johnson N, Weintraub S, Mesulam M, Rademakers R, Chakraverty S, Cruchaga C, Morris JC, Goate AM, Cairns NJ. TARDBP 3-prime-UTR variant in autopsy-confirmed frontotemporal lobar degeneration with TDP-43 proteinopathy. Acta Neuropath. 2009; 118:633–645. [PubMed: 19618195]
30. Luty AA, Kwok JBJ, Thompson EM, Blumsbergs P, Brooks WS, Loy CT, Dobson-Stone C, Panegyres PK, Hecker J, Nicholson GA, Halliday GM, Schofield PR. Pedigree with frontotemporal lobar degeneration-motor neuron disease and Tar DNA binding protein-43 positive neuropathology: genetic linkage to chromosome 9. BMC Neurology. 2008; 8:32. [PubMed: 18755042]
31. Renton AE, Majounie E, Waite A, Simón-Sánchez J, Rollinson S, Gibbs JR, Schymick JC, Laaksovirta H, van Swieten JC, Myllykangas L, Kalimo H, Paetou A, Abramzon Y, Remes AM, Kaganovitch A, Scholz SW, Duckworth J, Ding J, Harmer DW, Hernandez DG, Johnson JO, Mok K, Ryten M, Trabzuni D, Guerreiro RJ, Orrell RW, Neal J, Murray A, Pearson J, Jansen IE, Sondervan D, Seelaar H, Blake D, Young K, Halliwell N, Callister JB, Toulson G, Ricahrdson A, Gerhard A, Snowden J, Mann D, Neary D, Nalls MA, Peuralinna T, Jansson L, Isoviita VM, Kalvorinne AL, Hölttä-Vuori M, Ikonen E, Sulkava R, Benatar M, Wuu J, chio A, Restagno G, Borghero G, Sabatelli M, The ITALSGEN Consortium, Heckerman D, Rogaeva E, Zinman L, Rothstein JD, Sendtner M, Drepper C, Eichler EE, Alkan C, Abdullaev Z, Pack SD, Dutra A, Pak E, Hardy J, Singleton A, Williams NM, Heutink P, Pickering-Brown S, Morris HR, Tienari PJ, Traynor BJ. A hexanucleotide repeat expansion in *C9ORF72* is the cause of chromosome 9p21-linked ALS-FTD. Neuron. 2011; 72:257–268. [PubMed: 21944779]
32. Josephs KA, Whitwell JL, Jack CR, Parisi JE, Dickson DW. Frontotemporal lobar degeneration without lobar atrophy. Arch Neurol. 2006; 63:1632–1638. [PubMed: 17101834]
33. Kersaitis C, Holliday GM, Xuereb JH, Pamphlett R, Bak TH, Hodges JR, Kril JJ. Ubiquitin-positive inclusions and progression of pathology in frontotemporal dementia and motor neurone disease identifies a group with mainly early pathology. Neuropathol Appl Neurobiol. 2006; 32:83–91. [PubMed: 16409556]
34. Mirra SS, Heyman A, McKeel D, Sumi SM, Crain BJ, Brownlee LM, Vogel FS, Hughes JP, van Belle G and Berg L. The consortium to establish a registry for Alzheimer's disease (CERAD). Part II Standardization of the neuropathologic assessment of Alzheimer's disease. Neurology. 1991; 41:479–486. [PubMed: 2011243]
35. Jellinger KA, Bancher C. Neuropathology of Alzheimer's disease: a critical update. J Neural Transm. 1998; 54:77–95.
36. Newell KL, Hyman BT, Growden JH, Hedley-Whyte ET. Application of the National Institute on Aging (NIA)-Reagan Insitute criteria for the neuropathological diagnosis of Alzheimer's disease. J Neuropathol Exp Neurol. 1999; 58:1147–1155. [PubMed: 10560657]
37. Hyman BT, Phelps CH, Beach TG, Bigio EH, Cairns NJ, Carillo MC, Dickson DW, Duyckaerts C, Frosch MP, Masliah E, Mirra SS, Nelson PT, Schneider JA, Thal DR, Theis B, Trojanowski JQ, Vinters HV, Montine TJ. National Insitute on Aging-Alzheimer's Association Guidelines for the neuropathological assessment of Alzheimer's disease. Alzheimer & Dem. 2012; 8:1–13.
38. Braak H, Alafuzoff I, Arzberger T, Kretzschmar H, Del Tredici K. Staging of Alzheimer disease-associated neurofibrillary pathology using paraffin sections and immunocytochemistry. Acta Neuropathol. 2006; 112:389–404. [PubMed: 16906426]
39. Duyckaerts C, Hauw JJ, Bastenaire F, Piette F, Poulain C, Rainsard V, Javoy-Agid F, Berthaux P. Laminar distribution of neocortical senile plaques in senile dementia of the Alzheimer type. Acta Neuropathol. 1986; 70:249–256. [PubMed: 3766125]

40. Yaguchi M, Fujita Y, Amari M, Takatama M, Al-Sarraj S, Leigh PN, Okamoto K. Morphological differences of intraneural ubiquitin positive inclusions in the dentate gyrus and parahippocampal gyrus of motor neuron disease with dementia. Neuropathol. 2004; 24:296–301.
41. Davidson Y, Kelley T, Mackenzie IRA, Pickering Brown S, Du Plessis D, Neary D, Snowden JS, Mann DMA. Ubiquinated pathological lesions in frontotemporal lobar degeneration contain TAR DNA-binding protein, TDP-43. Acta Neuropathol. 2007; 113:521–533. [PubMed: 17219193]
42. Matsumoto S, Udaka F, Kameyama M, Kusaka H, Itoh H, Imai T. Subcortical neurofibrillary tangles, neuropil threads and argentophilic glial inclusions in corticobasal degeneration. Clin Neuropath. 1996; 15:209–214.
43. Armstrong RA, Cairns NJ, Lantos PL. A quantitative study of the pathological lesions in neocortex and hippocampus of 12 patients with corticobasal degeneration. Exp Neurol. 2000; 163:348–356. [PubMed: 10833308]
44. Yamada T, McGeer PL, McGeer EG. Appearance of paired nucleated tau-positive glia in patients with progressive supranuclear palsy brain tissue. Neurosci Lett. 1992; 135:99–102. [PubMed: 1371861]
45. Ikeda K, Akiyama H, Kondo H, Haga C, Tanno E, Tokuda T, Ikeda S. Thorn-shaped astrocytes: possibly secondarily induced tau-positive glial fibrillary tangles. Acta Neuropathol. 1995; 90:620–625. [PubMed: 8615083]
46. Komori T. Tau positive glial inclusions in progressive supranuclear palsy, corticobasal degeneration and Pick's disease. Brain Pathol. 1999; 9:663–679. [PubMed: 10517506]
47. Probst A, Tolnay M. Argyrophilic grain disease, a frequent and largely underestimated cause of dementia in old patients. Rev Neurol. 2002; 158:155–165. [PubMed: 11965171]
48. Pirici D, Vandenberghe R, Rademakers R, Dermant B, Cruts M, Vennekens K, Cuijt I, Lubke U, Centerick C, Martin JJ, Van Broeckhoven C, Kumar-Singh S. Characterization of ubiquinated intraneuronal inclusions in a novel Belgian frontotemporal lobar degeneration family. J Neuropath Exp Neurol. 2006; 65:289–301. [PubMed: 16651890]
49. Hatanpaa KJ, Bigio EH, Cairns NJ, Womack KB, Weintraub S, Morris JC, Foong C, Xiao GH, Hladik C, Mantanona TY, White CL. TAR DNA-binding protein 43 immunohistochemistry reveals extensive neuritic pathology in FTLD-U: A Midwest-Southwest Consortium for FTLD-U study. J Neuropathol Exp Neurol. 2008; 67:271–279. [PubMed: 18379440]
50. Armstrong RA. Correlations between the morphology of diffuse and primitive β-amyloid (Aβ) deposits and the frequency of associated cells in Down's syndrome. Neuropath Appl Neurobiol. 1996b; 22:527–530.
51. Armstrong RA, Lantos PL, Cairns NJ. Spatial correlations between the vacuolation, prion protein deposits, and surviving neurons in the cerebral cortex in sporadic Creutzfeldt-Jakob disease. Neuropathol. 2001; 21:266–271.
52. Armstrong RA, Ironside J, Lantos PL, Cairns NJ. A quantitative study of the pathological changes in the cerebellum of 15 cases of variant Creutzfeldt-Jakob disease. Neuropathol Appl Neurobiol. 2009; 35:36–45. [PubMed: 19187059]
53. Snedecor, GW.; Cochran, WG. Statistical Methods. Ames, Iowa USA: Iowa State University Press; 1980.
54. Neumann M, Kwong LK, Lee EB, Kremmer E, Flately A, Xu Y, Forman MS, Troost D, Kretzschmar HA, Trojanoswki JQ, Lee VMY. Phosphorylation of S409/410 of TDP-43 is a consistent feature in all sporadic and familial forms of TDP-43 proteinopathies. Acta Neuropathol. 2009; 117:137–149. [PubMed: 19125255]
55. Hasegawa M, Arai T, Nonaka T, Kametani F, Yoshida M, Hashizume Y, Beach TG, Buratti E, Baralle F, Morita M, Nakano I, Oda T, Tsuchiya K, Akiyama H. Phosphorylated TDP-43 in frontotemporal lobar degeneration and amyotrophic lateral sclerosis. Annals of Neurol. 2008; 64:60–70.
56. Olive M, Janve A, Moreno D, Gamez J, Torrejon-Escritano B, Ferrer I. TAR DNA-binding protein 43 accumulation in protein aggregate myopathies. J Neuropathol Exp Neurol. 2009; 68:262–273. [PubMed: 19225410]
57. Schwab C, Arai T, Hasegawa M, Akiyama H, Yu S, McGeer PL. TDP-43 pathology in familial British dementia. Acta Neuropathol. 2009; 118:303–311. [PubMed: 19283396]

58. Armstrong RA, Carter D, Cairns NJ. A quantitative study of the neuropathology of 32 sporadic and familial cases of frontotemporal lobar degeneration (FTLD) with TDP-43 proteinopathy (FTLD-TDP). Neuropathol Appl Neurobiol. 2012; 38:25–38. [PubMed: 21696412]

59. Minamu M, Mizutani T, Kawanishi R, Suzuki Y, Mori H. Neuronal expression of alpha B crystalline in cerebral infarction. Acta Neuropathol. 2003; 105:549–554. [PubMed: 12734661]

60. Pierucci A, de Oliveira AL. Increased sensory neuron apoptotic death two weeks after peripheral axonotomy in C57BL/6J mice compared to A/J mice. Neurosci Lett. 2006; 396:127–131. [PubMed: 16359790]

61. Kato S, Hirano A, Umahara T, Wena JF, Herz F, Ohama E. Ultrastructural and immunohistochemical studies on ballooned cortical neurons in Creutzfeldt-Jakob disease: expression of alpha-B-crystallin, ubiquitin and stress response protein-27. Acta Neuropathol. 1992; 84:443–448. [PubMed: 1332365]

62. Goedert M, Clavaguera F, Tolnay M. The propagation of prion-like protein inclusions in neurodegenerative diseases. Trends in Neurosciences. 2010; 33:317–325. [PubMed: 20493564]

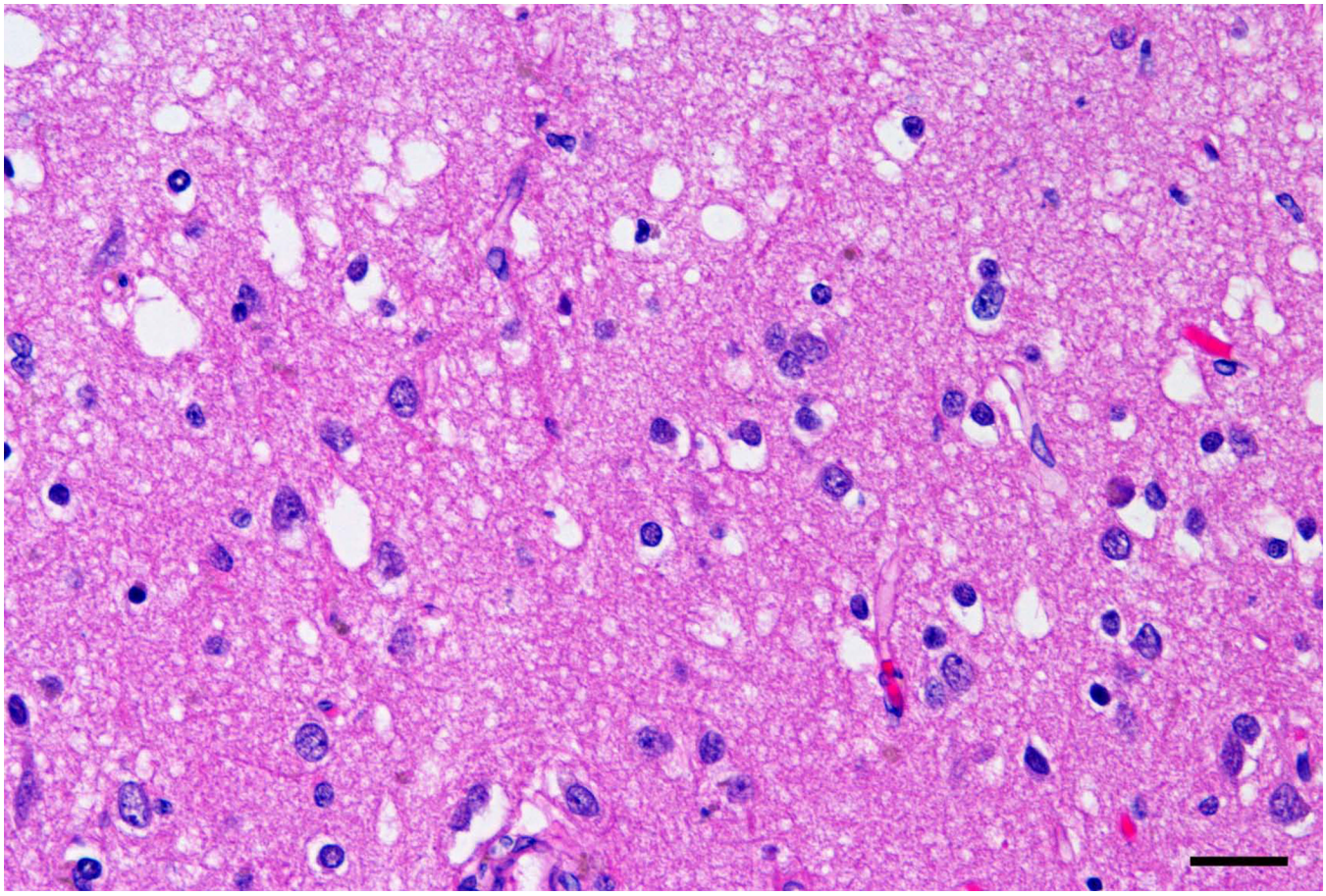

Fig 1.
Vacuolation in lamina II of the inferior temporal gyrus (ITG) in a case of frontotemporal lobar degeneration with TDP proteinopathy (FTLD-TDP) (H/E, bar = 20μm).

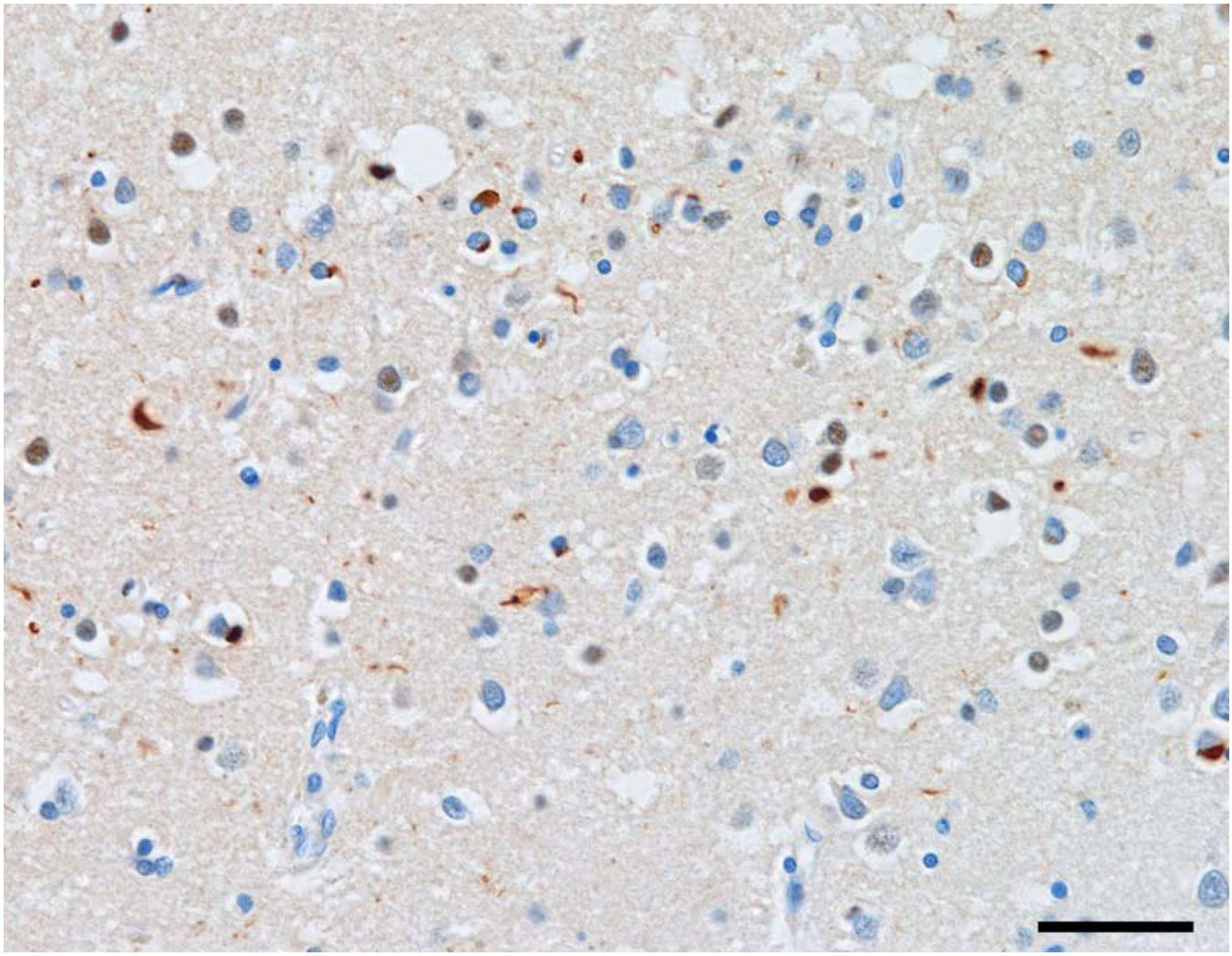

Fig 2.
TDP-43-immunoreactive inclusions in laminae II/III of the inferior temporal gyrus (ITG) in a case of frontotemporal lobar degeneration with TDP proteinopathy (FTLD-TDP) (TDP-43 immunohistochemistry, bar = 20μm).

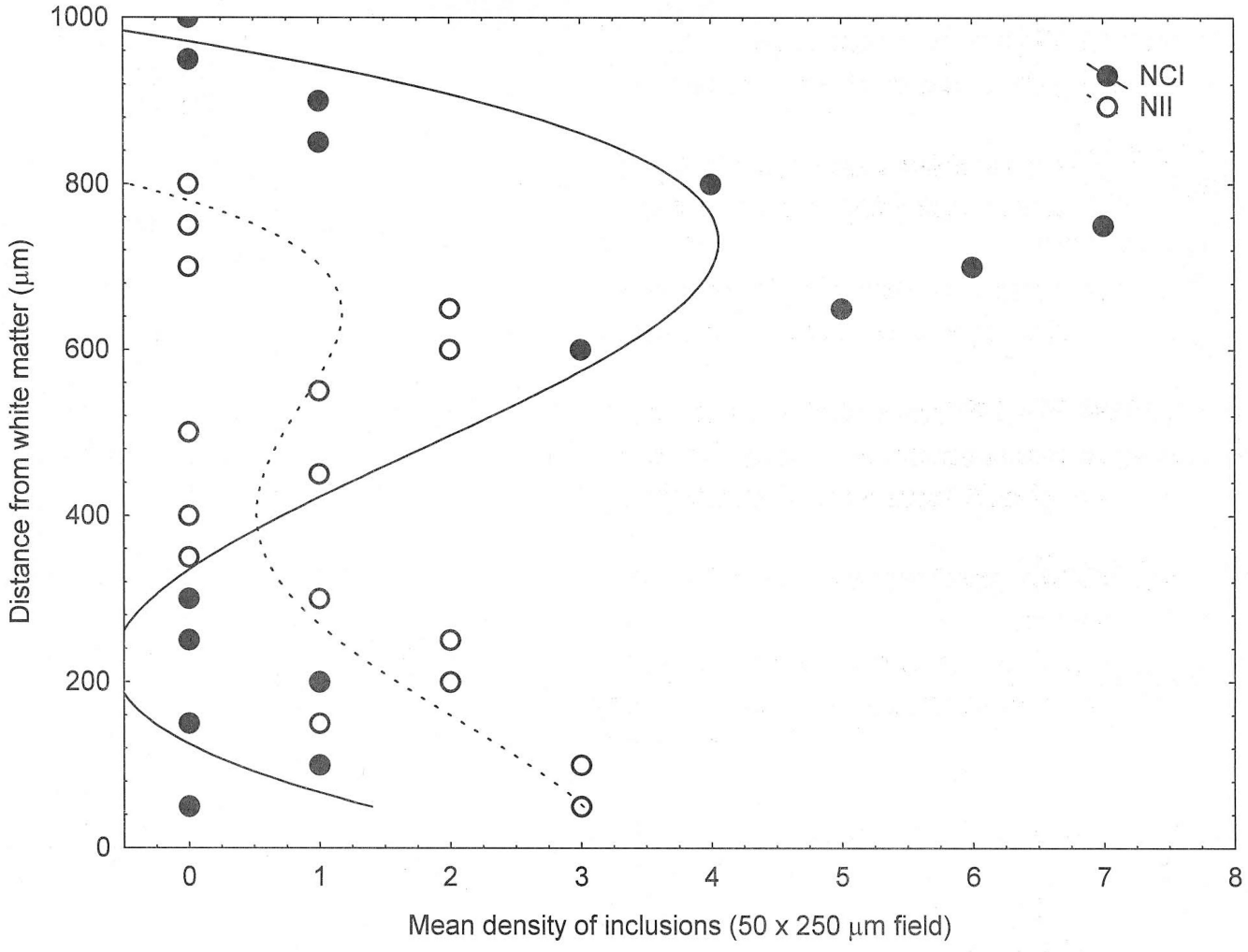

Fig 3.

Examples of the distribution of the neuronal cytoplasmic inclusions (NCI) and neuronal intranuclear inclusions (NII) in the middle frontal gyrus (MFG) of a case of frontotemporal lobar dementia with TDP-43 proteinopathy (FTLD-TDP). Curve of best fit: NCI, third order polynomial ($r = 0.70$, $P < 0.001$); NII, third-order polynomial ($r = 0.65$, $P < 0.01$).

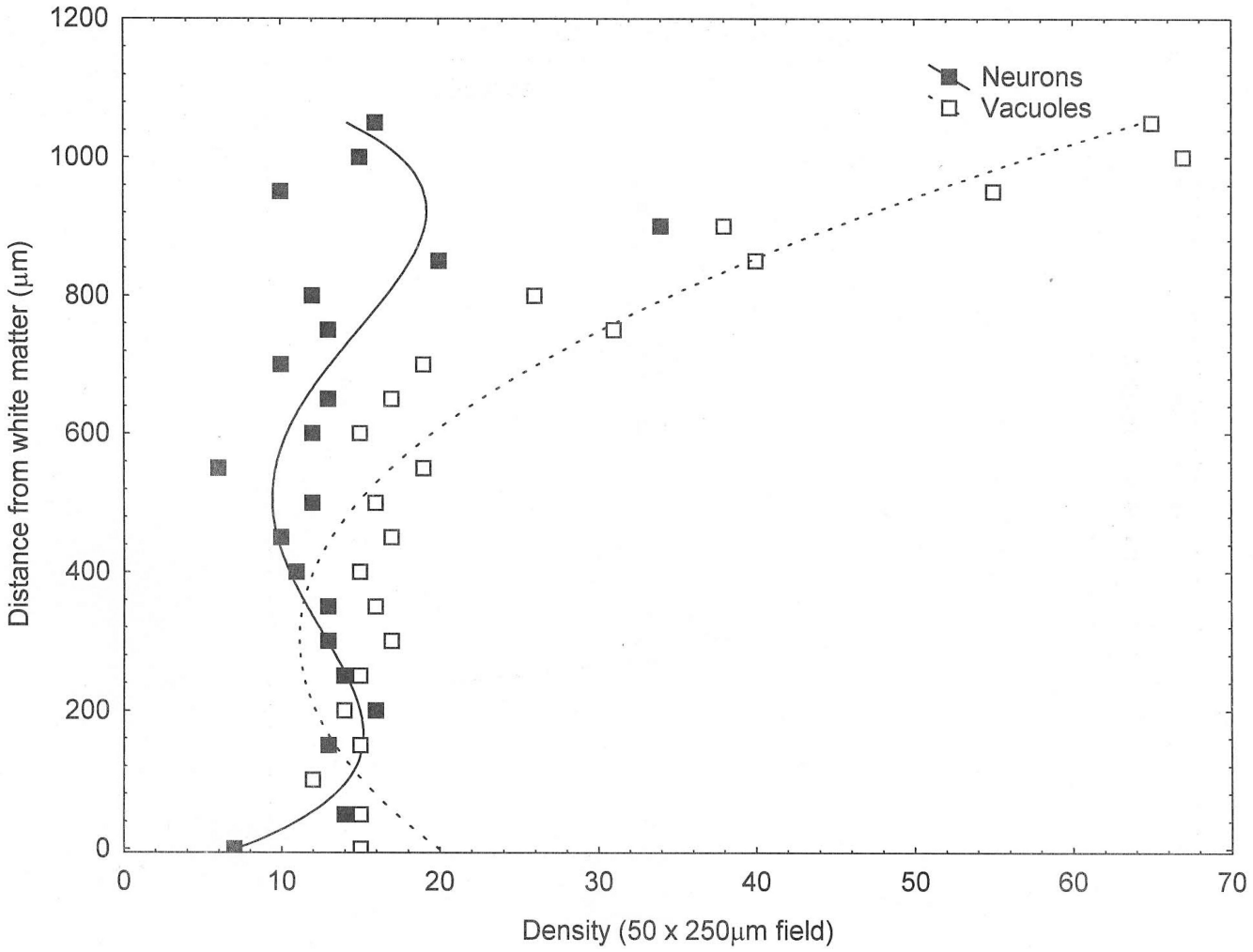

Fig 4.

Examples of the distribution of the surviving neurons and vacuolation in the middle frontal gyrus (MFG) in a case of frontotemporal lobar dementia with TDP-43 proteinopathy (FTLD-TDP). Curve of best fit: Surviving neurons, fourth-order polynomial ($r = 0.0.61$, $P < 0.01$); Vacuolation, second order polynomial ($r = 0.96$, $P < 0.001$).

Table 1

Demographic features, gross brain weight (BW), Braak tangle stage, and disease subtype of the ten cases of frontotemporal lobar degeneration with TDP-43 proteinopathy (FTLD-TDP).

Case	Centre	Sex	Onset	Death	Duration	BW	Braak stage	Assigned ST
A	H	F	80	88	8	1035	III	2
B	H	M	73	79	6	1180	II	3
C	V	F	-	82	-	940	0	1
D	V	M	69	72	3	-	0	2
E	V	M	66	71	5	1230	II	3
F	V	F	55	70	15	-	III	1
G *	V	M	70	71	1	1140	IV	2
H	P	M	61	65	4	1100	II	2
I	P	M	-	76	-	1440	III	1
J	P	M	61	64	3	1330	I	2

Abbreviations: H = Harvard Brain Tissue Resource Center, V = Vancouver General Hospital, P = Department of Pathology, University of Pittsburgh, M = Male, F = Female, Disease onset, age at death, and disease duration are given in years, BW = Brain weight (gm), Braak stage represents staging of Alzheimer disease-associated neurofibrillary pathology, ST = previously assigned disease subtype according to Cairns et al (2007).

(-)= data not available,

* Case with associated motor neuron disease (MND)

Table 2

Results of the polynomial curve-fitting procedure for each histological feature features

Case	Feature	MFG	ITG	PHG
A	NCI	4, 0.45 * (U)	1, 0.45 *(U)	3, 0.61 *(U)
	GI	4, 0.80 **(L)	NS	3, 0.67 *(L)
	NII	-	2, 0.60 *(L)	3, 0.66 *(L)
	EN	1,0.61 *(U)	4,0.42 *(U = L)	-
	SN	1,0.72 ***(U)	NS	NS
	V	4,0.77(U)	1,0.59 *(U)	2,0.96 *(U)
	DN	-	-	-
	GL	1,0.88 **(L)	1,0.80 ***(L)	1,0.82 ***(L)
B	NCI	NS	-	3, 0.48 *(U)
	GI	-	NS	3, 0.67 *(L)
	NII	-	2, 0.60 *(L)	3, 0.66 *(L)
	EN	1,0.61 *(U)	4,0.42 *(U = L)	-
	SN	1,0.72 ***(U)	NS	NS
	V	4,0.77(U)	1,0.59 *(U)	2,0.96 ***(U)
	DN	-	-	-
	GL	1,0.88 **(L)	1,0.80 ***(L)	1,0.82 ***(L)
C	NCI	-	NS	-
	GI	-	-	4, 0.61 *(L)
	NII	-	-	-
	EN	NS	NS	-
	SN	1,0.52 **(U)	3,0.64 ** (U = L)	1,0.70 ***(U)
	V	1,0.79 ***(U)	3,0.70 **(U)	4,0.72 **(U = L)
	DN	4,0.76 ***(U)	2.0.49 *(L)	2,0.73 **(U = L)
	GL	1,0.86 **(L)	1,0.73 ***(L)	4,0.63 *(L)
D	NCI	3,0.70 ***(U)	4,0.52 *(U)	4, 0.59 **(U)
	GI	NS	-	-
	NII	3,0.48 *(L)	-	1,0.49 *(L)
	EN	4,0.47 *(U)	NS	-
	SN	4,0.62 **(U)	3,0.59 **(U)	4,0.56 **(U = L)
	V	4,0.91 ***(U)	3,0.88 ***(U)	3,0.92 ***(U)
	DN	-	-	-
	GL	1,0.82 **(L)	1,0.67 ***(L)	2,0.69 ***(L)
E	NCI	NS	4,0.90 ***(U)	4, 0.49 *(U = L)
	GI	1, 0.42 *(L)	-	-
	NII	NS	NS	-

Case	Feature	MFG	ITG	PHG
	EN	NS	2,0.42 *(L)	NS
	SN	NS	NS	2,0.49 *(U)
	V	3,0.90 ***(U)	2,0.57 **	4,0.64 **(U)
	DN	-	3,o.38 *(U)	-
	GL	1,0.59 ***(L)	1,0.69 ***(L)	3,0.78 ***(L)
F	NCI	-	-	-
	GI	-	4,0.57 *(L)	-
	NII	3,0.52 *(L)	3.0.65 *(L)	3,0.54 *(L)
	EN	-	-	-
	SN	4,0.53 **(U)	3,0.83 ***(U)	4,0.44 *(U = L)
	V	2,0.97 ***(U)	3,0.90 ***(U)	2,0.91 ***(U)
	DN	3,0.59 *(U)	2,0.78 ***(U)	3,0.57 ** (U = L)
	GL	1,0.85 **(L)	3,0.88 ***(L)	1,0.86 **(L)
G	NCI	-	4,0.56 **(U = L)	-
	GI	-	-	-
	NII	NS	4,0.54 **(L)	NS
	EN	2,0.46 **(L)	4,0.39 *(U)	3,0.41 *(U = L)
	SN	4,0.39 *(U)	3,0.41 *(U = L)	3,0.87 ***(U)
	V	2,0.92 **(U)	4,0.88 **(U)	3,0.90 **(U)
	DN	-	NS	3,0.80 **(L)
	GL	1,0.78 ***(L)	3,0.88 ***(L)	2,0.83 ***(L)
H	NCI	3,0.69 ***(U)	3,0.73 ***(U)	3,0.85 ***(U)
	GI	-	-	-
	NII	-	-	-
	EN	NS	2,0.40 *(L)	-
	SN	NS	4,0.80 ***(U)	NS
	V	4,0.60 **(U)	2,0.75 **(U)	2,0.79 ***(U)
	DN	-	-	-
	GL	1,0.88 ***(L)	1,0.84 ***(L)	1,0.95 ***(L)
I	NCI	1,0.43 *(L)	NS	4,0.71 ***(U)
	GI	-	-	-
	NII	4,0.82 ***(L)	NS	NS
	EN	4,0.59 **(L)	NS	1,0.50 **(L)
	SN	3,0.70 ***(U = L)	4,0.63 **(U = L)	4,0.57 ***(U)
	V	2,0.76 ***(U)	2,0.42 *(U = L)	4,0.67 ***(U = L)
	DN	3,0.72 ***(L)	-	-
	GL	1,0.91 ***(L)	1,0.78 ***(L)	1,0.83 ***(L)

Case	Feature	MFG	ITG	PHG
J	NCI	3,0.61 **(U)	NS	NS
	GI	-	-	-
	NII	NS	4,0.54 **(L)	NS
	EN	-	4,0.55 *(U)	NS
	SN	NS	NS	2,0.70 ***(U = L)
	V	2,0.84 ***(U)	2,0.86 ***(U)	4,0.95 **(U)
	DN	NS	3,0.78 ***(L)	-
	GL	1,0.84 ***(L)	1,0.80 ***(L)	2,0.73 **(L)

(NCI = Neuronal cytoplasmic inclusions, GI = Glial inclusions, NII = Neuronal intranuclear inclusions, DN = Dystrophic neurites, EN = Abnormally enlarged neurons, V = Vacuolation, SN = Surviving neurons, GL = Glial cell nuclei) in each cortical gyrus. The first figure of each entry is the order of polynomial fitted to the data (1 = linear, 2 = quadratic, 3 = cubic, 4 = quartic), the second figure is the statistical significance of the fitted curve (*P < 0.05, **P < 0.01, ***P < 0.001, NS = no significant curve fitted the data), and the third letter in parentheses, whether a density peak was located in the upper (U) or lower (L) cortex (- indicates insufficient density of a histological feature to quantify its distribution).

Table 3

Summary of the various types of distribution exhibited by the histological features

		Unimodal distribution		Bimodal distribution			
Lesion	**N**	**Upper cortex**	**Lower cortex**	**Upper > lower**	**Upper = lower**	**Upper < lower**	**NS**
NCI	23	7	1	5	3	1	6
GI	6	1	1	0	0	3	1
NII	21	1	6	0	1	5	8
DN	13	2	2	4	2	2	1
EN	20	2	6	1	1	0	10
SN	30	4	0	9	8	1	8
V	30	8	0	17	4	0	1
GL	30	0	28	0	0	2	0

(NCI = Neuronal cytoplasmic inclusions, GI = Glial inclusions, NII = Neuronal intranuclear inclusions, DN = Dystrophic neurites, EN = Abnormally enlarged neurons, V = Vacuolation, SN = Surviving neurons, GL = Glial cell nuclei) across the cortex in gyri of the frontal and temporal lobe in ten cases of sporadic frontotemporal lobar dementia with TDP-43 proteinopathy (FTLD-TDP) (N = number of gyri with sufficient densities of lesions to study laminar distribution). Where a bimodal distribution is present, data indicate whether the density peak in the upper laminae was greater, equal to, or smaller than the density peak in the lower laminae, NS = no significant change in density from pia mater to white matter.

Neuropathol Appl Neurobiol. Author manuscript; available in PMC 2014 June 01.

Table 4

Relationship between the distribution of TDP-43-immunoreactive inclusions, disease duration, and Braak stage in frontotemporal lobar dementia with TDP-43 proteinopathy (FTLD-TDP). Data show the frequency of gyri in which collectively, the TDP-43-immunoreactive inclusions exhibited a unimodal or a bimodal distribution, NS = No significant change in abundance across the cortex.

		Laminar distribution	
Variable	**Categories**	**Unimodal**	**Bimodal**
Disease duration	1 – 4	11	5
(years)	5 – 8	4	11
	15	1	5
Braak stage	0/1	10	4
	2	4	6
	3	5	13
	4	0	3

Chi-square (χ^2) contingency table tests: Disease duration $\chi^2 = 10.63$ (4DF, $P < 0.05$), Braak score $\chi^2 = 9.46$ (6DF, $P > 0.05$), Disease subtype $\chi^2 = 3.71$ (4DF, $P > 0.05$)

Table 5

Comparison of the distribution of the neuronal cytoplasmic inclusions (NCI), neuronal intranuclear inclusions (NII), and dystrophic neurites (DN) based on quantitative data with previously assigned disease subtypes of frontotemporal lobar degeneration with TDP proteinopathy (FTLD-TDP) classified according to the consensus scheme of Cairns et al. [10].

		Frequency of laminar distribution			
Inclusion	**Subtype**	**Upper cortex**	**Lower cortex**	**Bimodal distribution**	**NS**
NCI	1	1	1	0	1
	2	6	0	5	2
	3	2	0	1	0
NII	1	0	2	2	2
	2	0	2	5	3
	3	2	0	0	3
DN	1	4	0	0	0
	2	1	0	2	2
	3	3	1	1	1

NS = No significant change in abundance across the cortex.

Neuropathol Appl Neurobiol. Author manuscript; available in PMC 2014 June 01.

Table 6

Frequency of correlations (Pearson's 'r') between the densities of histological features

		Frequency of significant correlations		
Variables	**N**	**Positive correlation**	**Negative correlation**	**NS**
NCI/GI	8	0	0	8
NCI/NII	18	0	0	18
NCI/DN	10	1	0	9
NCI/EN	19	0	0	19
NCI/SN	24	9	0	15
NCI/V	24	4	0	20
NCI/GL	23	3	1	19
GI/NII	9	1	0	8
GI/DN	6	0	0	6
GI/EN	9	0	0	9
GI/SN	12	1	0	11
GI/V	11	0	0	11
GI/GL	12	3	0	8
NII/DN	11	0	0	11
NII/EN	16	0	0	16
NII/SN	21	0	0	21
NII/V	21	0	0	21
NII/GL	22	5	0	17
DN/EN	10	0	0	10
DN/SN	15	0	0	15
DN/V	15	1	1	13
DN/GL	15	0	0	15
EN/SN	21	0	0	21
EN/V	21	1	1	19
EN/GL	20	0	1	19
SN/V	31	14	0	17
SN/GL	30	0	8	22
V/GL	30	0	12	18

(NCI = Neuronal cytoplasmic inclusions, GI = Glial inclusions, NII = Neuronal intranuclear inclusions, DN = Dystrophic neurites, EN = Abnormally enlarged neurons, V = Vacuolation, SN = Surviving neurons, GL = Glial cell nuclei) across gyri of the frontal and temporal cortex from pia mater to white matter in ten cases of frontotemporal lobar dementia with TDP-43 proteinopathy (FTLD-TDP), N = number of gyri tested, NS = no significant correlations.